

Analysis of Type IV pilin in *Vibrio parahaemolyticus*

by

Chun-kit Shum

A thesis submitted to the Faculty of the University of Delaware in partial fulfillment of the requirements for the degree of Degree in Bachelor of Arts in Biological Sciences with Distinction


Spring 2022


© 2022 Chun-kit Shum
All Rights Reserved


Analysis of Type IV pilin in *Vibrio parahaemolyticus*

by

Chun-kit Shum

Approved:  _____
E. Fidelma Boyd, Ph.D.
Professor in charge of thesis on behalf of the Advisory Committee

Approved:  _____
Molly C. Sutherland, Ph.D.
Committee member from the Department of Department Name

Approved:  _____
Gary H. Laverty, Ph.D.
Committee member from the Board of Senior Thesis Readers

Approved: _____
Dana Veron, Ph.D.
Chair of the University Committee on Student and Faculty Honors

ACKNOWLEDGMENTS

I would not have been able to conduct and complete this project without the guidance of those around me. I entered the University of Delaware curious about how research is performed, a curiosity driven by my high school biology teacher Mr. McDowell who often talked about his research. Dr. Boyd has allowed me into her lab and show me the world of research. She has guided my experience in the lab and helped me mature as a researcher. I am entirely grateful for everything she has done for me. I also want to thank Dr. Sutherland and Dr. Lavery for their guidance on my project. Without their advice and encouragement, I would have faced many more hardships.

I also want to give my thanks to my lab mentor Dr. Jessica Tague. Jess has been guiding me since my sophomore year, for 2 and a half years she has watched over me. She has patiently taught me many skills and techniques and encouraged me since the very beginning, I could not have asked for a better mentor.

I want to thank those in Dr. Boyd's lab: Katherine Boas, Soham Mangesh Bhide, Heather Thomas, and Jackson Andrews for helping with my research and creating a positive learning environment.

Additionally, I also want to thank my family and friends. I would not be who I am without everyone, I am grateful for every moment since I stepped into the lab 4 years ago, Thank you.

TABLE OF CONTENTS

LIST OF TABLES	vi
LIST OF FIGURES	vii
ABSTRACT	ix
1 INTRODUCTION	1
1.1 Introduction to <i>Vibrio</i>	1
1.2 <i>Vibrio parahaemolyticus</i>	1
1.3 Type IV pilin system	3
1.4 Biofilm.....	5
1.5 Aims of the Study	5
2 METHODS AND MATERIALS	7
2.1 Bioinformatics	7
2.2 Construction of the $\Delta VP2423$ mutant.....	7
2.3 Growth pattern analysis	13
2.4 Swimming assay	13
2.5 Swarming assay	14
2.6 Capsule polysaccharide production assay	14
2.7 Biofilm formation assay	15
3 RESULTS.....	16
3.1 Construction of the $\Delta VP2423$ mutant.....	16
3.2 Characterizing of $\Delta VP2423$ and $\Delta mshA$	17
3.3 Biofilm formation.....	21
4 DISCUSSION.....	24
4.1 $\Delta VP2423$ compared to $\Delta mshA$	24
4.2 Future directions	24
REFERENCES	25
A BACTERIAL STRAINS AND PLASMIDS.....	29
B PRIMERS USED IN MUTANT MAKING PROCESS	30

LIST OF TABLES

Table 1	A list of bacterial strains and plasmids used during the mutant making process	29
Table 2	The table above displays the sequence of the primers used in the production of the $\Delta VP2423$ mutant.....	30

LIST OF FIGURES

- Figure 1. Structure of a Type IV pilin system. Connected to the inner membrane is a platform protein and ATPase protein. In the periplasm is the alignment protein complex surrounding a pilus made of major pilin proteins. The pilus exits the outer membrane through the Secretin protein channels. The top of the pilus are minor pilin proteins 4
- Figure 2. A model depicting the location of primers designed in the gene deletion process. Primer set AB and CD were designed in-frame of the *VP2423* gene and are 500 bps. Flanking primers were designed outside the AB forward to CD reverse primer regions 8
- Figure 3. Diagram of the AB and CD DNA fragments ligated into the digested pDS132 plasmid via Gibson assembly 8
- Figure 4. Agarose gel image to confirm the successful transformation of pDS132 Δ *VP2423* into *E.coli* DH5 α . The positive control, indicated by “+”, is wild type gDNA and has a length of 1156-bp. *E.coli* DH5 α pDS132 Δ *VP2423* cells in lane 1 and lane 2 and has a length of 1000-bp. The negative control is indicated by the “-“ symbol.....9
- Figure 5. Agarose gel image to confirm the successful transformation of pDS132 Δ *VP2423* into *E.coli* β 2155 λ *pir*. The positive control, indicated by “+”, is wild type gDNA and has a length of 1156bp. *E.coli* β 2155 λ *pir* pDS132 Δ *VP2423* cells indicated by “1” and “2” and has a length of 1000bp. The negative control is indicated by the “- “ symbol..... 10
- Figure 6. Agarose gel image to confirm the insertion of the pDS132 Δ *VP2423* into *V. parahaemolyticus* RIMD2210633 genome. Two set primers were used in this screening: AD primers and Flanking primers. The positive control, indicated by “+”, is wild type gDNA and has a length of 1156bp when using AD primers, and 1843bp when using the flanking primers. *V. parahaemolyticus* RIMD2210633 pDS132 Δ *VP2423* is indicated by “1” with a length of 1000bp when using the AD primers, and no band when using the flanking primers. “2 -10” Are colonies that failed to incorporate the vector into their genome. The negative control is indicated by the “- “ symbol..... 11
- Figure 7. Plate image of a double-crossover colonies grown on 3% NaCl LB + 10% Sucrose plates. The healthy colony is depicted as having a creamy color, while the soupy colony appears sickly or soupy 12

- Figure 8. Agarose gel image to confirm the deletion of the pDS132 Δ VP2423 from *V. parahaemolyticus* genome. Two set primers were used in this screening: AD primers and Flanking primers. The positive control, indicated by “+”, is wild type gDNA and has a length of 1156bp when using AD primers, and 1843-bp when using the flanking primers. *V. parahaemolyticus* Δ VP2423 is indicated by “1” with a length of 1000-bp when using the AD primers, and 1687-bp when using the flanking primers. The negative control is indicated by the “-“symbol 12
- Figure 9. Gel image of Δ VP2423 mutant screening. Positive control is represented by the “+” symbol, and negative control by the “-“symbol. The lower band confirms the deletion of the VP2423 gene 16
- Figure 10. Growth curves of *V. parahaemolyticus* RIMD2210633 (positive control), Δ VP2423, and Δ mshA were grown in lysogeny broth (LB) with 3% NaCl for 24 hours at 37°C. The OD_{595nm} was measured every hour for 24 hours. A logarithmic graph was used to display the growth of the strains 17
- Figure 11. Swimming assays. Swimming media was made using lysogeny broth with 3% NaCl and 0.6% Agar. The plates were inoculated and incubated at 37°C for 24 hours. RIMD2210633 served as the positive control. ** P < 0.01 18
- Figure 12. Swarming assays. *V. parahaemolyticus* RIMD2210633, Δ VP2423, Δ mshA, and Δ opaR were grown on heart infusion with 2% NaCl and 1.5% Agar. The plates were spot inoculated and incubated at 30°C for 48 hours 19
- Figure 13. Capsule polysaccharide assays (CPS) wild type, Δ VP2423, Δ mshA and Δ opaR were grown in heart infusion with 1.5% Agar, 100mM calcium chloride and Congo red dye. The plates were spot inoculated and incubated at 30°C for 48 hours 21
- Figure 14. Biofilm formation assay. The strains were done in duplicates, side by side. From left to right wild type, Δ VP2423, Δ msha, and negative control 22
- Figure 15. Quantification of biofilm formation. *V. parahaemolyticus* RIMD2210633 (positive control), Δ VP2423, and Δ mshA were grown in lysogeny broth with 3% NaCl at 37°C for 24 hours. The growth wells were washed with 1x phosphate buffered saline and stained with 0.1% crystal violet for 30 minutes. The biofilm was solubilized using dimethyl sulfoxide, and the OD_{595nm} of the samples were measured 23

ABSTRACT

Vibrio parahaemolyticus is a Gram-negative bacterium that is ubiquitous in the marine environment and is also a human pathogen that when ingested induces gastroenteritis. This bacterium expresses on its surface rod like hair-like appendages called pili. Pili are important for bacterial adherence to surfaces such as shellfish and human cells. The *V. parahaemolyticus* genome contains several different pili, but the most common class of pili is the type IV. In *V. parahaemolyticus*, four type IV pili have been identified, two of which are TAD Caulobacter Pilin Assembly (CPA) type IV pilins, as well as the mannose-sensitive hemagglutinin (MSHA), and the chitin-regulated pilus (ChiRP/Pil). MSHA pilin is required for adherence, biofilm production, and twitching motility. CHiRP is required for adherence to chitin surfaces and natural transformation for DNA uptake. This study focused on the characterization of one of the two TAD CPA type IV pilins, the TAD1 CPA type IV pilin. In this work, a non-functional TAD1 mutant strain was constructed by deleting the pilin protein encoded by the *VP2423* gene creating a $\Delta VP2423$ mutant. The mutant strain was then characterized using growth pattern analysis and phenotypic assays: swimming and swarming assays, capsule polysaccharide production, and biofilm formation. The mutant strain grew similar to wild type in all these assays.

Chapter 1

INTRODUCTION

1.1 Introduction to *Vibrio*

Vibrio is a genus of Gram-negative bacteria commonly found in brackish and marine waters. Species in this genus tend to have specific salinity preferences, for example, *Vibrio cholerae* prefers 0.5-6% NaCl (11). *Vibrio* are facultative anaerobes meaning that they can live in environments rich or deprived of oxygen (20). Members of this family tend to grow quickly with some species having double times as short as 10 minutes (9). *Vibrio* are important in the ecosystem because they can take part in chitin degradation, a very abundant polymer. Additionally, some species are known to be pathogenic to humans and sea dwellers. Ingesting *V. cholerae* can lead to cholera, a water rich diarrhea, while species like *V. parahaemolyticus* can lead to inflammatory diarrhea. Both *V. cholerae* and *V. parahaemolyticus* are mesophiles growing optimally at warmer temperatures (30°C-37°C), thus many *Vibrio* proliferate in the warmer summer months. Cases of *Vibrio* infection are increasing every year due to climate change resulting in rising sea water temperature (4).

1.2 Introduction to *Vibrio parahaemolyticus*

Vibrio parahaemolyticus is a halophilic bacterium found in estuaries and in intertidal zones. *V. parahaemolyticus* has a salinity preference of 3% but can grow

between 1-6% (25). Infectious in nature, these bacteria serve as the leading cause of bacterial seafood-borne gastroenteritis in the world. Human infection is caused through the consumption of raw and poorly prepared seafood, mainly shellfish (22). Infections are especially severe during warmer months as temperature and salinity show a strong correlation with *V. parahaemolyticus* proliferation (10).

Historically speaking, *V. parahaemolyticus* was first identified in 1950s in Osaka, Japan during an outbreak of gastroenteritis. The consumption of sardines led to 272 people being infected, resulting in 20 deaths. The symptoms of gastroenteritis were recorded as diarrhea, cramps, vomiting, nausea, headache, chill, and fever (22). Starting in 1969, cases of *V. parahaemolyticus* outbreak were beginning to appear outside of Japan, with the first case in the United States in 1971. In 2011, 30,000 infections were reported worldwide and since then infections have been seen throughout Europe, Asia, and Africa (4).

V. parahaemolyticus is characterized as having both polar and lateral flagella, which are long appendages used for motility. The polar flagellum is a singular appendage that helps the bacteria move in liquid environments, known as swimming motility. The lateral flagella are numerous and allow for motility on solid surfaces called swarming motility. An important aspect to *V. parahaemolyticus*' lifecycle is the ability to form a biofilm. A biofilm is a static 3-dimensional structure of cells that bacteria produce when attached to surfaces (11). *V. parahaemolyticus* expresses pili, numerous short hair-like appendages on it's surface that can assist in twitching motility, adherence, DNA uptake, and biofilm production. Pili production is an

important virulence factor that allows the bacteria to switch from a planktonic state to an infectious sessile state (17).

1.3 Type IV pilin system

Pili are numerous short hair like appendages found on the surface of many types of bacteria. These appendages are 1-4 μ m, thin (50-80 \AA), flexible, and strong allowing bacteria to interact with their environment (6). Pili can help bacteria adhere to surfaces, which is very useful when the environment fluctuates. One of the most common types of pilins is the type IV pilin. Structurally, type IV pilins are made up of an assembly ATPase, retraction ATPase, and a platform protein. On the inner membrane are the alignment proteins, and crossing the plasma membrane are secretin, major pilin, and minor pilin proteins (5). Hydrolysis of ATP allows for conformational change in the assembly ATPase which leads to structural changes in the alignment proteins. This opens the alignment proteins enough for major pilin proteins to enter and build onto the existing pilus causing it to grow and extend. The pilus builds up from the inner membrane and through the outer membrane utilizing a protein channel developed from secretin (13). When the pilus makes contact with a surface, the tension produced causes conformational change in the machinery, in which the assembly ATPase gets replaced by the retraction ATPase, reversing the process, and retracting the pilus (6).

The type IV pilin system is found in both Gram-positive and Gram-negative bacteria (13). The system is classified into 2 distinct classes: T4aP, and T4bP. The

difference between these classes lies in their structure. T4aP pilins having a shorter pilin and its genes are scattered throughout its genome. T4bP pilins are overall longer and the genes required to make them are clustered together on the genome (2). For T4a pilins there are two known types that are commonly found in *Vibrio* species, the chitin-regulated pilus (ChiRP/Pil) and the mannose-sensitive hemagglutinin (MSHA) (2). In *V. cholerae*, a type IV pilin system is essential for virulence, known as the toxin co-regulated pilus (TCP), and the MSHA and Pil systems are known to influence adherence, biofilm production, twitching motility, and DNA uptake.

In *V. parahaemolyticus* the type IV pilin system is not well studied, but four distinct type IV pilin structures have been identified. Some of these pilins have not been characterized, and more research will be needed to fully understand their place in the *V. parahaemolyticus* biological system.

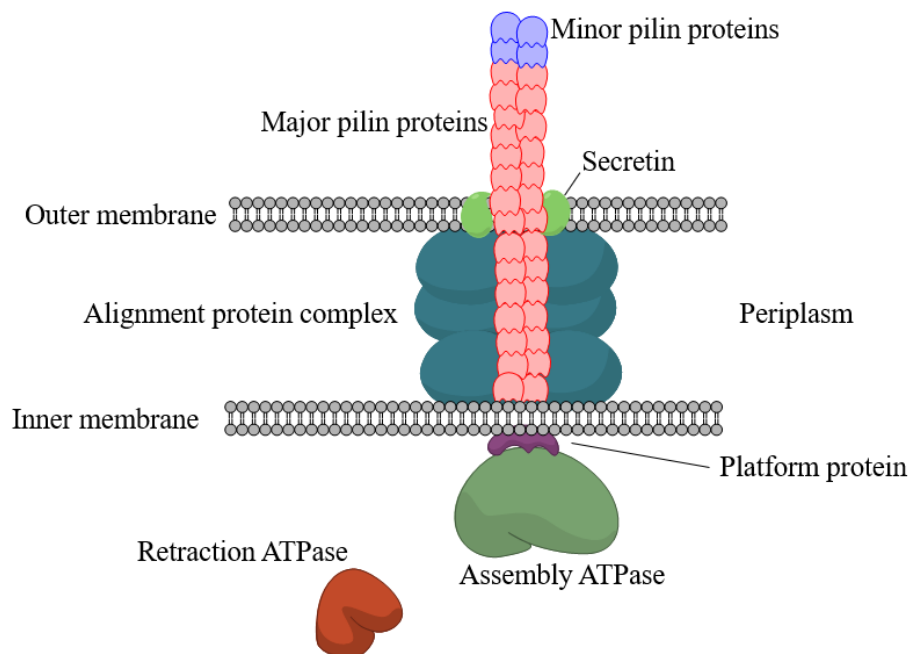


Figure 1. Structure of a Type IV pilin system. Connected onto the inner membrane is a platform protein and ATPase protein. In the periplasm is the alignment protein complex surrounding a pilus made of major pilin proteins. The pilus exits the outer membrane through the Secretin protein channels. The top of the pilus are minor pilin proteins.

1.4 Biofilm

Biofilm formation is an important virulence factor for many bacteria. Biofilms are a matrix of cells, polysaccharide, glycoproteins, and carbohydrates that can serve as a protective structure (11). Biofilm formation starts when planktonic cells swimming through their environment make contact with a surface. When this happens, the cells adhere to the surface using their pili and begin to twitch (movement through repetitive extension and retraction of one's pili) (22). Twitching motility allow for the compaction and conglomeration of bacteria until the cells reach a higher cell density, leading to the expression of capsule polysaccharides and sometime virulence genes. Capsule production in *V. parahaemolyticus* is controlled by quorum sensing. Quorum sensing is a form of cell-to-cell communication that utilizes the surveillance of signaling molecules to determine cell density. In high cell density conditions, the bacterium produces capsule, an essential component of biofilms (26) (15).

1.5 Aims of the study

As previously mentioned, type IV pili are not well studied in *V. parahaemolyticus* and some of the known pili have yet to be characterized, for

example, the TAD1 Caulobacter pilus assembly (CPA) type IV pilin (13). The goal of this study is to determine whether the TAD1 CPA pilin is required for capsule production and biofilm formation. A $\Delta mshA$ *V. parahaemolyticus* strain, which has a deleted mannose-sensitive hemagglutinin type IV pilin and has been previously characterized in the lab, will be used as a control for the assays. Through my research, I aim to determine whether my TAD1 mutant strain, $\Delta VP2423$, had reduced capsule and biofilm formation. I am also interested if other factors that contribute to biofilm formation, such as growth and motility will be affected upon deletion of the *VP2423* gene.

Chapter 2

METHODS AND MATERIALS

2.1 Bioinformatics

Utilizing the National Center for Biotechnology Information's (NCBI) database of *V. parahaemolyticus* RIMD2210633, the TAD1 pilin protein was identified as ORF *VP2423*. The gene sequence was downloaded as a GenBank file and viewed in SnapGene Viewer. A BLAST search was conducted with the *VP2423* protein product to look for homologous proteins in other *Vibrio* species.

2.2 Construction of the $\Delta VP2423$ mutant

Splicing by overlap extension, PCR, and homologous recombination was used to construct an in-frame deletion of TAD1. Construction of the $\Delta VP2423$ mutant began by designing three sets of primers from the *V. parahaemolyticus* RIMD2210633 genome: AB, CD, and the flanking primers. The AB and CD fragments are roughly 500 bp each and flank the gene of interest upstream (AB fragment) and downstream regions (CD fragment). The flanking primers were designed outside the AB and CD regions as seen on Figure 2. The AB and CD primers allow for the creation of two segments of DNA. When ligated together, these two fragments produce a DNA fragment with the in-frame deletion of the *VP2423* gene. The AB and CD DNA fragments were replicated through PCR and extracted with a gel extraction kit.

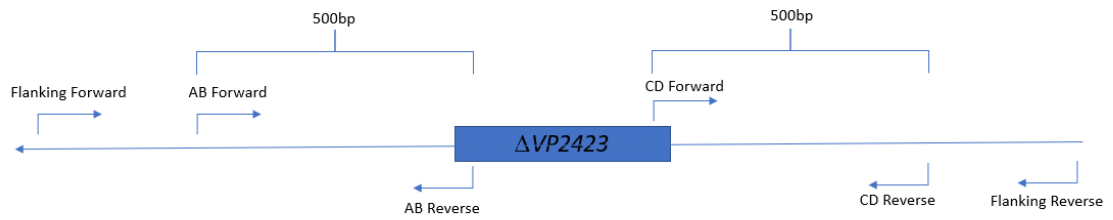


Figure 2. Diagram depicting the location of primers designed in the gene deletion process. Primer set AB and CD were designed in-frame of the *VP2423* gene and are 500 base pairs long. Flanking primers were designed outside the AB forward to CD reverse primer regions.

Next the pDS132 vector is purified with a plasmid purification kit and linearized with the restriction enzyme *SacI*. As seen on Figure 3. Gibson assembly is utilized to ligate the AB and CD DNA fragment with the linearized pDS132 vector.



Figure 3. Diagram of the AB and CD DNA fragments being ligated onto the digested pDS132 plasmid via Gibson assembly.

The annealed vector is then transformed into an *Escherichia coli* DH5 α strain. The successful transformation into *E.coli* DH5 α (Figure 4) allow for the replication of this vector.

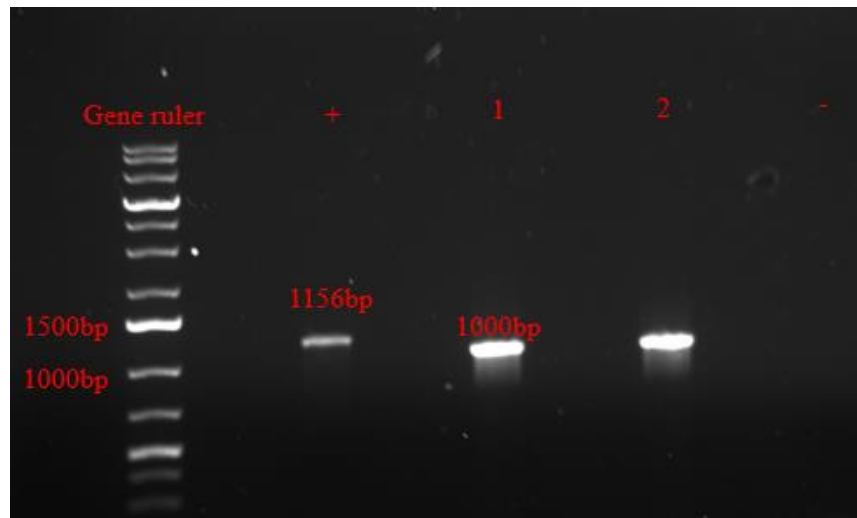


Figure 4. A screening image to confirm the successful transformation of pDS132 Δ VP2423 into *E.coli* DH5 α . The positive control, indicated by “+”, is wild type gDNA and has a length of 1156bp. *E.coli* DH5 α pDS132 Δ VP2423 cells are indicated by “1” and “2” and has a length of 1000bp. The negative control is indicated by the “-“symbol.

Afterwards the pDS132 Δ VP2423 vector is transformed into *E.coli* β 2155 λ pir (Figure 5.), a diaminopimelic acid auxotroph. *E.coli* β 2155 λ pir pDS Δ VP2423 was then be conjugated with wild type. To accomplish this *E.coli* β 2155 λ pir pDS Δ VP2423 is then spread onto 1% NaCl LB + 100 μ L DAP plates along with wild type. Next day this plate is quarter streaked onto a 3% NaCl LB plate with full chloramphenicol plate. The 3% NaCl promotes the growth of RIMD2210633, the CM selects for cells with the plasmid, and the lack of DAP selects against β 2155 λ pir.

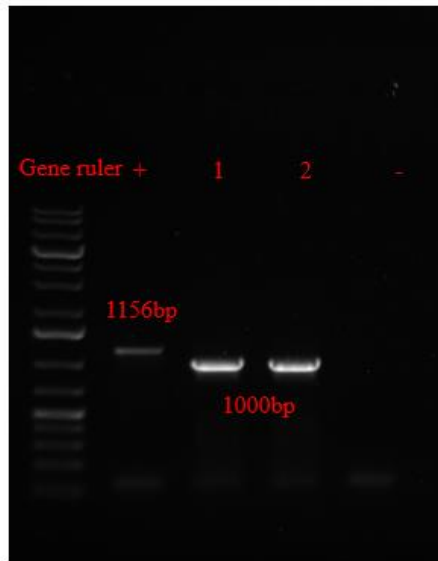


Figure 5. Agarose gel image to confirm the successful transformation of pDS132 Δ VP2423 into *E.coli* β 2155 λ pir. The positive control, indicated by “+”, is wild type gDNA and has a length of 1156bp. *E.coli* β 2155 λ pir pDS132 Δ VP2423 cells indicated by “1” and “2” and has a length of 1000bp. The negative control is indicated by the “-” symbol.

In Figure 6, to check if the vector has been inserted into the genome, a screening is conducted to observe the crossing over of the plasmid with the chromosome (homologous recombination). Healthy cells are screened with two sets of primers, the AD, and flanking primers. Because the distance between the flanking primers is too long when the pDS vector is incorporated into the genome, there should be no band. But the AD fragment is smaller, so we would expect to yield a band measuring 1000bp.

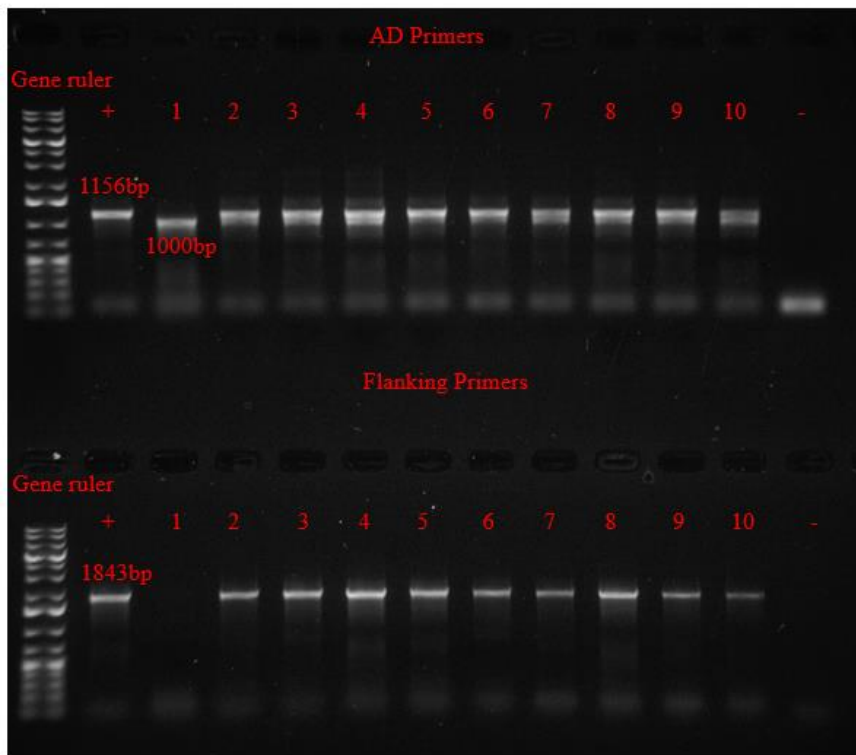


Figure 6. Agarose gel image to confirm the insertion of the pDS132 Δ VP2423 into wild type. Two set primers were used in this screening: AD primers and Flanking primers. The positive control, indicated by “+”, is wild type gDNA and has a length of 1156bp when using AD primers, and 1843bp when using the flanking primers. *V. parahaemolyticus* pDS132 Δ VP2423 is indicated by “1” with a length of 1000bp when using the AD primers, and no band when using the flanking primers. “2 -10” Are colonies that failed to incorporate the vector into their genome. The negative control is indicated by the “-” symbol.

To induce a double crossover event, the cultures of the positive colonies were serially diluted and streaked onto 3% NaCl LB + 10% sucrose plates. The lack of CM and the exposure to sucrose promotes the deletion of the plasmid from the chromosome. This is because without CM the chloramphenicol resistance gene, *cat*, is no longer necessary. Additionally, the *sacB* gene on the pDS132 plasmid leads to the

production of Levan sucrose, a substance that is toxic to the cells. As seen on Figure 8, a screening of healthy cells (refer to Figure 7) is done with both the AD and flanking primers. Bands from both primer sets indicates the deletion of the *VP2423* gene from the RIMD2210633 genome.

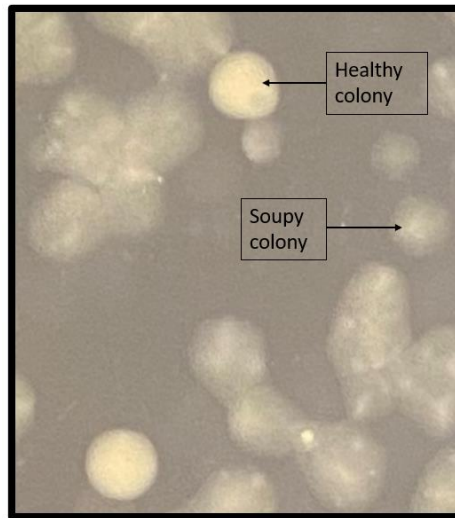


Figure 7. Image of a double-crossed colonies grown on 3% NaCl LB + 10% Sucrose plates. The healthy colony is depicted as having a creamy color, while the soupy colony appears sickly or soupy.

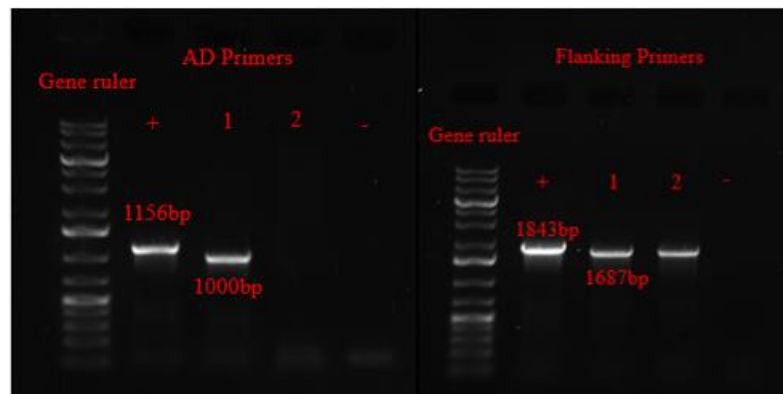


Figure 8. Agarose gel image to confirm the deletion of the pDS132 Δ VP2423 from *V. parahaemolyticus* genome. Two set primers were used in this screening: AD primers and Flanking primers. The positive control, indicated by “+”, is wild type gDNA and has a length of 1156-bp when using AD primers, and 1843-bp when using the flanking primers. *V. parahaemolyticus* Δ VP2423 is indicated by “1” with a length of 1000-bp when using the AD primers, and 1687-bp when using the flanking primers. The negative control is indicated by the “-“symbol.

2.3 Growth Curve

For growth curve assays, strains of interests are streaked out onto LB 3% NaCl plates and incubated at 37°C overnight. *V. parahaemolyticus* RIMD2210633 will be used as a positive control. An isolated colony from each plate is incubated into LB 3% NaCl overnight with shaking at 37°C for 16 hours. On the next day, using a microplate 200 μ L of 3% NaCl LB were added into each well along with 5 μ L of culture. A blank of LB 3% NaCl is used as a blank and control. The plate is loaded onto a Tecan reader with an incubation temperature of 37°C. The plate is read every hour for 24 hours with shaking set to 1000 seconds before each read.

2.4 Swimming assay

For swimming assays, strains of interests are streaked onto 3% NaCl LB plates and incubated at 37°C overnight. *V. parahaemolyticus* RIMD2210633 is used as a positive control, and a *V. parahaemolyticus* Δ rp*oN* is used as a negative control, which was previously shown to be immotile. Swimming media plates are prepared using LB 3% NaCl with 0.6% agar. Each plate is inoculated with a single strain once and

incubated at 37°C for 24 hours. After 24 hours the plates are measured from the furthest diameter of the colony.

2.5 Swarming assay

For swarming assays, strains of interests are streaked out onto 3% NaCl LB plates and incubated at 37°C overnight. *V. parahaemolyticus* RIMD2210633 and $\Delta opaR$, a mutant *V. parahaemolyticus* strain that has a hyper swarming phenotype, will be used as a positive control. Swarming media is made from heart infusion broth, 2% NaCl, and 1.5% Agar and used to spot colonies on the surface of the plate (each plate contains 3-6 inoculants) and incubated at 30°C for 48 hours. After 48 hours the plates are observed for swarming phenotype, and imaged.

2.6 Capsule polysaccharide (CPS) assay

For CPS assays, strains of interests are streaked out onto 3% NaCl LB plates and incubated at 37°C overnight. *V. parahaemolyticus* RIMD2210633 will be used as a positive control, and *V. parahaemolyticus* $\Delta opaR$ will be used as a negative control, OpaR is essential for CPS production. Capsule polysaccharide media contains heart infusion broth, 1.5% agar, and 50mg of Congo red dye along with 5mL of 100mM calcium chloride. Strains are inoculated on the surface of the plate, 3-6 spot inoculants are on each plate and incubated at 30°C for 48 hours. Afterwards the plates are observed for capsule polysaccharide and imaged.

2.7 Biofilm assay

For biofilm assays, strains of interests are streaked out onto 3% NaCl LB plates and incubated at 37°C overnight. *V. parahaemolyticus* RIMD2210633 is used as a positive control, and *V. parahaemolyticus* $\Delta rpoN$ is used as a negative control. Isolated colonies from these plates will be used to make 3% NaCl LB overnight cultures, incubated in a shaking incubator for 16 hours at 37°C. On the day of the assay, the strip wells are sterilized with ultraviolet light for 15 minutes. In each well 200 μ L of fresh 3% NaCl LB broth, along with 5 μ L of the overnight culture are added. A control containing only 3% NaCl are in the last 2 wells. The wells are incubated for 24 hours at 37°C. On the next day, the supernatant is removed, and each well is washed with 220 μ L of 1x phosphate buffered saline (PBS). Then, 220 μ L of 0.1% crystal violet is added to each well and incubated at room temperature for 30 minutes. The stained wells are washed with 1x PBS once again. The strip well is imaged and observed for biofilm. In the next step the biofilm is solubilized with 220 μ L of dimethyl sulfoxide (DMSO). A spectrometer is used to read the OD_{595nm} level of each sample, DMSO serves as the blank for this assay.

Chapter 3

RESULTS

3.1 Construction of a TAD1 mutant by deletion of the *VP2423* gene

The ORF *VP2423* encodes the TAD1 pilin protein and is therefore essential for TAD1 production. Using splicing by overlap extension, PCR, and homologous recombination a *VP2423* deletion was made. In fig. 9, the $\Delta VP2423$ mutant was confirmed by the double cross screening yielding bands with the AD and flanking primers. An additional screening is done after the production of the mutant to confirm the 156-bp *VP2423* gene is deleted.

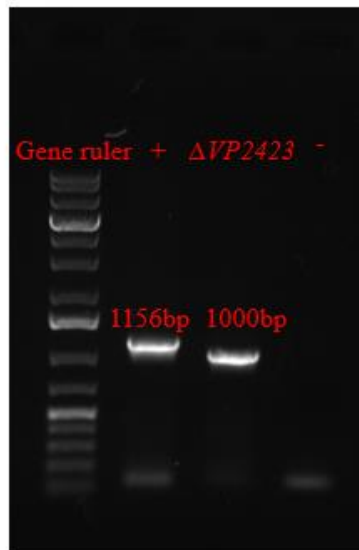


Figure 9. Gel image of $\Delta VP2423$ mutant screening. Positive control is represented by the “+” symbol, and negative control by the “-” symbol. The lower band confirms the deletion of the *VP2423* gene.

3.2 Characterizing $\Delta VP2423$ and $\Delta mshA$

Characterization of the $\Delta VP2423$ mutant will begin with a growth curve comparing the strain to that of RIMD2210633, and $\Delta mshA$. The $\Delta mshA$ mutant serve as a control for the remaining assays. Analysis of the growth curve incubated at 37°C in 3% NaCl LB show no growth defect in the $\Delta VP2423$ or $\Delta mshA$ mutant. Both mutant strains grew similar to wild type RIMD2210633. The resulting data (Figure 10.) show RIMD2210633 hitting stationary phase around the 22-hour mark and ended the 24-hour incubation with an OD_{595nm} of 1.06. $\Delta VP2423$ hit stationary phase around the 20-hour mark and ended with an OD_{595nm} of 1.02. $\Delta mshA$ hit stationary phase around the 19-hour mark and ended with an OD_{595nm} of 1.04.

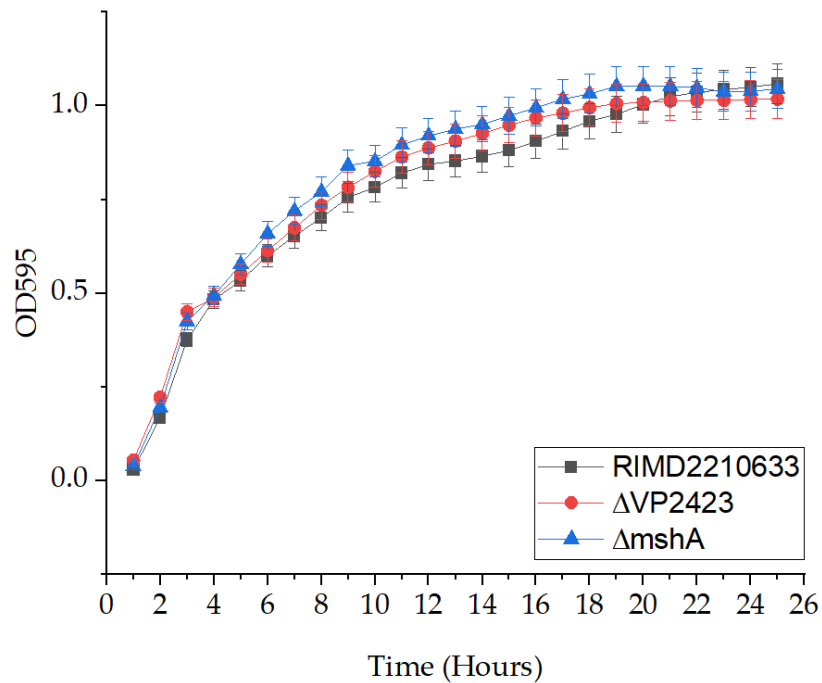


Figure 10. Growth curve analysis of *V. parahaemolyticus* RIMD2210633 (positive control), $\Delta VP2423$ and $\Delta mshA$. These strains were grown in LB 3% NaCl for 24

hours. The OD_{595nm} was measured every hour for 24 hours at 37°C. A logarithmic graph was used to display the growth of the strains.

Swimming motility is a phenotype characterized by the existence of polar flagellum. This is a rod like appendage that allow for motility in liquid media. If the TAD1 CPA or MSHA systems impacted polar flagellum, we would expect to see a defect in swimming in the mutants. In this case, the assay was performed on wild type, $\Delta VP2423$, and $\Delta mshA$ strains. As seen in Figure 11, no swimming defects were observed. Wild type had an average swimming diameter of 78.6mm, $\Delta VP2423$ had an average swimming diameter of 74.675mm, and $\Delta mshA$ had an average swimming diameter of 69.392mm. Both the mutant strains' diameters were close to wild type (RIMD2210633), and the p-value was not statistically significant.

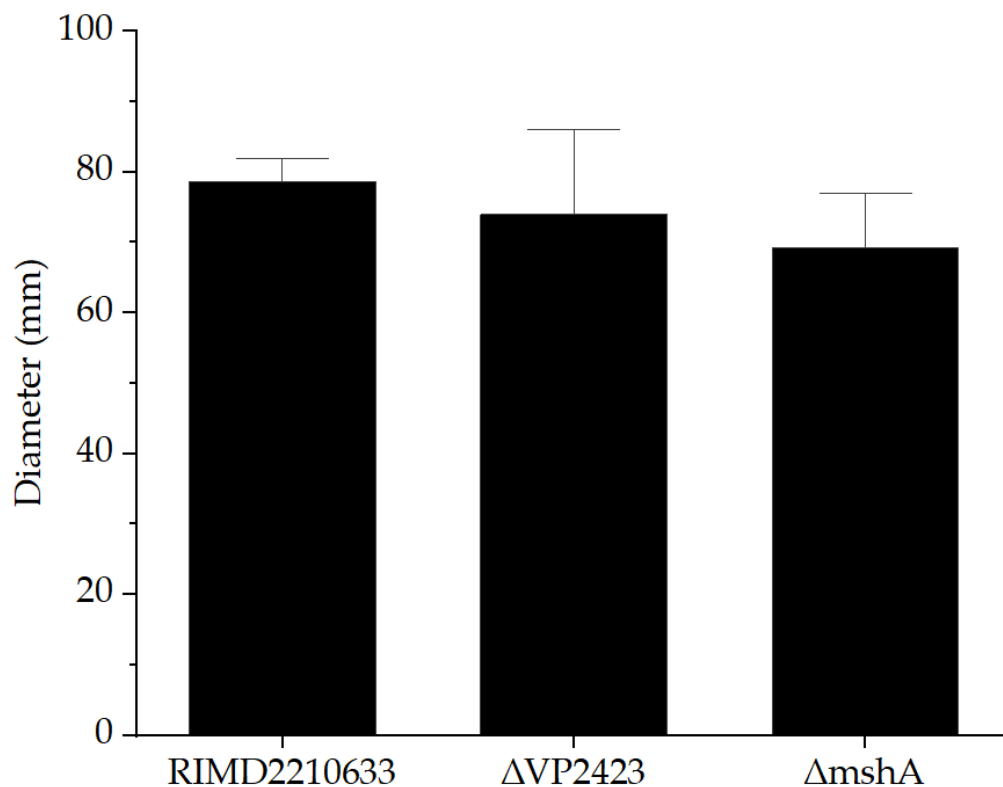
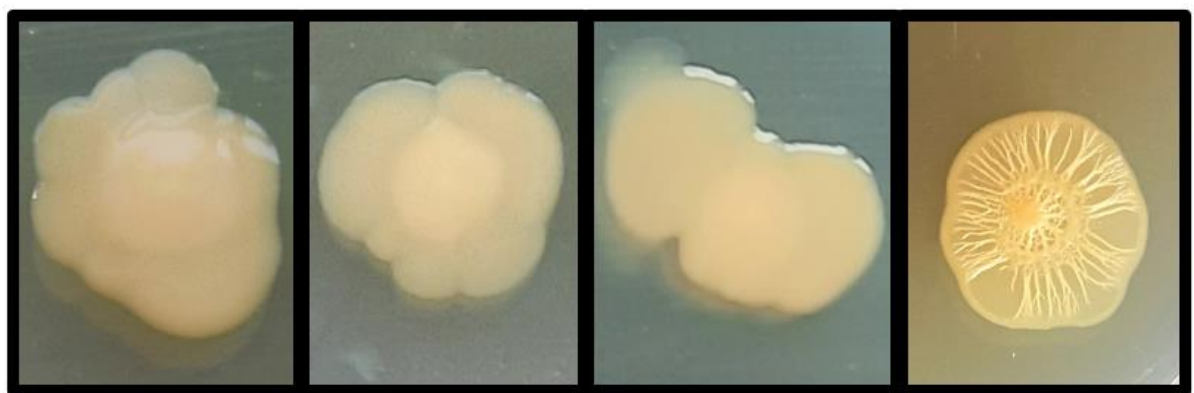


Figure 11. Swimming media was made using lysogeny broth with 3% NaCl and 0.6% Agar. The plates were inoculated and incubated at 37°C for 24 hours. RIMD2210633 served as the positive control. P-value was not statistically significant.

Swarming motility is carried out by the lateral flagella on solid surfaces. For this assay, I used the strains RIMD2210633, $\Delta VP2423$, $\Delta mshA$, and $\Delta opaR$.

RIMD2210633 was used as a positive control, while $\Delta opaR$ is a known as a hyper swarmer that is used as an additional positive control. Swarming is depicted as the cloud like expansion from the central colony. As seen in Figure 12, both $\Delta VP2423$ and $\Delta mshA$ exhibit a swarming phenotype, similar to the wild-type strain, but different to $\Delta opaR$. The results show that $\Delta VP2423$ and $\Delta mshA$ does not have a swarming defect and does not display a hyper-swarming phenotype.



RIMD2210633

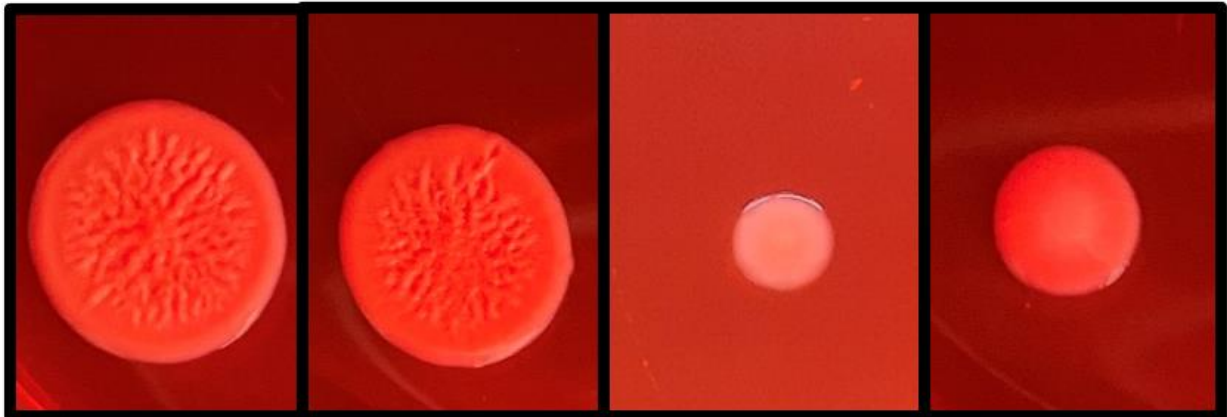
$\Delta VP2423$

$\Delta mshA$

$\Delta opaR$

Figure 12. *V. parahaemolyticus* RIMD2210633, $\Delta VP2423$, $\Delta mshA$, and $\Delta opaR$ were grown on heart infusion with 2% NaCl, and 1.5% Agar. The plates were spot inoculated and incubated at 30°C Celsius for 48 hours.

Capsule polysaccharide (CPS) is a surface structure on biofilm that serves to protect the bacterial community from environmental stress factors. As the name implies, this protective barrier is composed of various sugar molecules covalently bonded together (13). In the CPS assay, wild-type RIMD2210633 was used as a positive control, and $\Delta opaR$ as a negative control. A defect will give a smooth translucent colony as depicted by $\Delta opaR$ in Figure 13. CPS production can be indicated by the existence of a root like structure on the surface of the colony as depicted by RIMD2210633 in Figure 13. From this assay, we can see that $\Delta VP2423$ does not have a defect in CPS production as shown by its similarity to that of the wild-type strain. But $\Delta mshA$ is defective in capsule polysaccharide production indicated by its smooth and translucent morphology (Figure 13.)



RIMD2210633

$\Delta VP2423$

$\Delta mshA$

$\Delta opaR$

Figure 13. Capsule polysaccharide assay. *V. parahaemolyticus* RIMD2210633, $\Delta VP2423$, $\Delta mshA$ and $\Delta opaR$ were grown on heart infusion with 1.5% Agar, 100mM calcium chloride and Congo red dye. The plates were spot inoculated and incubated at 30°C for 48 hours.

3.3 Biofilm formation

As CPS is an essential part of biofilm development, a defect in CPS production tends to show a defect in biofilm and vice versa. To see if this remains true, $\Delta VP2423$ and $\Delta mshA$ were grown in a strip well for 24 hours at 37°C with RIMD2210633 as a positive control. After washing the 0.1% crystal violet off, purple rings can be observed by looking at the side of the strip wells (Figure 14). These rings are biofilm that have been stained by the crystal violet.



Figure 14. Biofilm formation assay. The strains were examined in duplicate, side by side. From left to right wild type, $\Delta VP2423$, $\Delta mshA$, and negative control.

When quantitatively measured through spectroscopy in Figure 15., $\Delta VP2423$ biofilm production ($OD_{595nm} = 1.72$) was similar to RIMD2210633 ($OD_{595nm} = 1.58$). But $\Delta mshA$ shows diminished biofilm production ($OD_{595nm} = 0.286$) indicating a defect in this characteristic. The data between $\Delta mshA$ and RIMD2210633 was statistically significant.

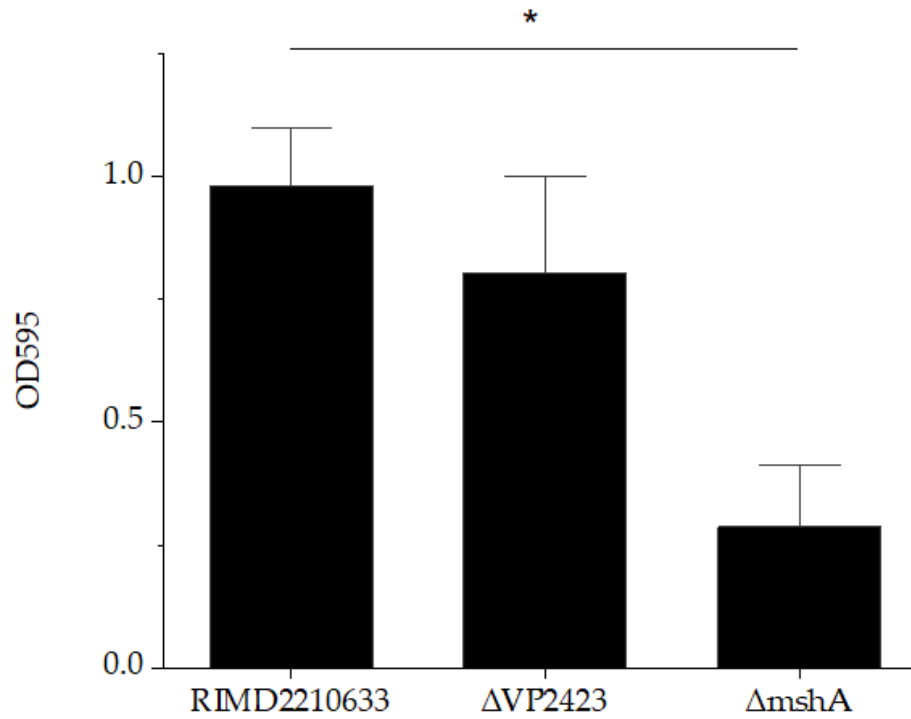


Figure 15. Quantification of biofilm formation. *V. parahaemolyticus* RIMD2210633 (positive control), $\Delta VP2423$, and $\Delta mshA$ were grown in lysogeny broth with 3% NaCl at 37°C for 24 hours. The growth wells were washed with 1x phosphate buffered saline and stained with 0.1% crystal violet for 30 minutes. The biofilm was solubilized using dimethyl sulfoxide, and the OD_{595nm} of the samples were measured.

Chapter 4 DISCUSSION

4.1 $\Delta VP2423$ compared to $\Delta mshA$

This study examined the biofilm and phenotypic characterization of the TAD1 and MSHA pilin. The $\Delta VP2423$ and $\Delta mshA$ mutant strains did not show any defects in growth or swimming and swarming motility. Additionally, $\Delta VP2423$ also did not have any defect in capsule polysaccharide or biofilm production. It is unlikely that the TAD1 pilin impacts lateral flagellum, polar flagellum, capsule polysaccharide, or biofilm production.

In comparison, $\Delta mshA$ did show a defect in capsule polysaccharide and biofilm production. The MSHA pilin system had previously been characterized to be able to control biofilm, adhesion, DNA uptake, and twitching motility (19). From this study we can confirm that the MSHA pilin system can at least regulate biofilm synthesis as the mutant showed defects in both capsule polysaccharide and biofilm production. This is consistent to the data collected by Shime-Hattori and her colleagues.

4.2 Future directions

This study has checked if the MSHA and TAD1 pilin system regulate swimming, swarming, capsule polysaccharide, and biofilm production. It is known that the Type IV pilin system is also capable of regulating DNA uptake, twitching motility, and adhesion. In the future, these other characteristics will have to be analyzed to see if they are regulated by MSHA or TAD1 CPA Type IV pilin system.

REFERENCES

1. Aagesen, A. M., Phuvasate, S., Su, Y. C., & Häse, C. C. (2013). Persistence of *Vibrio parahaemolyticus* in the Pacific oyster, *Crassostrea gigas*, is a multifactorial process involving pili and flagella but not type III secretion systems or phase variation. *Applied and environmental microbiology*, *79*(10), 3303–3305. <https://doi.org/10.1128/AEM.00314-13>
2. Aagesen, A. M., & Häse, C. C. (2012). Sequence analyses of type IV pili from *Vibrio cholerae*, *Vibrio parahaemolyticus*, and *Vibrio vulnificus*. *Microbial ecology*, *64*(2), 509–524. <https://doi.org/10.1007/s00248-012-0021-2>
3. Ashrafudoulla, M., Mizan, M., Park, H., Byun, K. H., Lee, N., Park, S. H., & Ha, S. D. (2019). Genetic Relationship, Virulence Factors, Drug Resistance Profile and Biofilm Formation Ability of *Vibrio parahaemolyticus* Isolated From Mussel. *Frontiers in microbiology*, *10*, 513. <https://doi.org/10.3389/fmicb.2019.00513>
4. Baker-Austin, C., Oliver, J.D., Alam, M. *et al.* *Vibrio* spp. infections. *Nat Rev Dis Primers* **4**, 1–19 (2018). <https://doi.org/10.1038/s41572-018-0005-8>
5. Chang, Y. W., Rettberg, L. A., Treuner-Lange, A., Iwasa, J., Søggaard-Andersen, L., & Jensen, G. J. (2016). Architecture of the type IVa pilus machine. *Science (New York, N.Y.)*, *351*(6278), aad2001. <https://doi.org/10.1126/science.aad2001>
6. Craig, L., Taylor, R. K., Pique, M. E., Adair, B. D., Arvai, A. S., Singh, M., Lloyd, S. J., Shin, D. S., Getzoff, E. D., Yeager, M., Forest, K. T., & Tainer, J. A. (2003). Type IV pilin structure and assembly: X-ray and EM analyses of *Vibrio cholerae* toxin-coregulated pilus and *Pseudomonas aeruginosa* PAK pilin. *Molecular cell*, *11*(5), 1139–1150. [https://doi.org/10.1016/s1097-2765\(03\)00170-9](https://doi.org/10.1016/s1097-2765(03)00170-9)
7. Floyd, K. A., Lee, C. K., Xian, W., Nametalla, M., Valentine, A., Crair, B., Zhu, S., Hughes, H. Q., Chlebek, J. L., Wu, D. C., Hwan Park, J., Farhat, A. M., Lomba, C. J., Ellison, C. K., Brun, Y. V., Campos-Gomez, J., Dalia, A. B., Liu, J., Biais, N., Wong, G., ... Yildiz, F. H. (2020). c-di-GMP modulates type IV MSHA pilus retraction and surface attachment in *Vibrio cholerae*. *Nature communications*, *11*(1), 1549. <https://doi.org/10.1038/s41467-020-15331-8>
8. Frischkorn, K. R., Stojanovski, A., & Paranjpye, R. (2013). *Vibrio parahaemolyticus* type IV pili mediate interactions with diatom-derived chitin and point to an unexplored mechanism of environmental persistence. *Environmental microbiology*, *15*(5), 1416–1427. <https://doi.org/10.1111/1462-2920.12093>

9. Froelich, B., Gonzalez, R., Blackwood, D., Lauer, K., & Noble, R. (2019). Decadal monitoring reveals an increase in *Vibrio* spp. concentrations in the Neuse River Estuary, North Carolina, USA. *PloS one*, *14*(4), e0215254. <https://doi.org/10.1371/journal.pone.0215254>
10. Hartwick, M. A., Urquhart, E. A., Whistler, C. A., Cooper, V. S., Naumova, E. N., & Jones, S. H. (2019). Forecasting Seasonal *Vibrio parahaemolyticus* Concentrations in New England Shellfish. *International journal of environmental research and public health*, *16*(22), 4341. <https://doi.org/10.3390/ijerph16224341>
11. Fu, X., Liang, W., Du, P., Yan, M., & Kan, B. (2014). Transcript changes in *Vibrio cholerae* in response to salt stress. *Gut pathogens*, *6*(1), 47. <https://doi.org/10.1186/s13099-014-0047-8>
12. Kelly M. T. (1982). Effect of temperature and salinity on *Vibrio* (*Beneckeia*) *vulnificus* occurrence in a Gulf Coast environment. *Applied and environmental microbiology*, *44*(4), 820–824. <https://doi.org/10.1128/aem.44.4.820-824.1982>
13. Ligthart, K., Belzer, C., de Vos, W. M., & Tytgat, H. (2020). Bridging Bacteria and the Gut: Functional Aspects of Type IV Pili. *Trends in microbiology*, *28*(5), 340–348. <https://doi.org/10.1016/j.tim.2020.02.003>
14. Morais, V., Dee, V., & Suárez, N. (2018). Purification of capsular polysaccharides of *Streptococcus pneumoniae*: Traditional and new methods. *Frontiers in Bioengineering and Biotechnology*, *6*. <https://doi.org/10.3389/fbioe.2018.00145>
15. Muhammad, M. H., Idris, A. L., Fan, X., Guo, Y., Yu, Y., Jin, X., Qiu, J., Guan, X., & Huang, T. (2020). Beyond Risk: Bacterial Biofilms and Their Regulating Approaches. *Frontiers in microbiology*, *11*, 928. <https://doi.org/10.3389/fmicb.2020.00928>
16. O'Boyle, N., Houeix, B., Kilcoyne, M., Joshi, L., & Boyd, A. (2013). The MSHA pilus of *Vibrio parahaemolyticus* has lectin functionality and enables TTSS-mediated pathogenicity. *International journal of medical microbiology : IJMM*, *303*(8), 563–573. <https://doi.org/10.1016/j.ijmm.2013.07.010>
17. Parveen, S., Jacobs, J., Ozbay, G., Chintapenta, L. K., Almuhaideb, E., Meredith, J., Ossai, S., Abbott, A., Grant, A., Brohawn, K., Chigbu, P., & Richards, G. P. (2020). Seasonal and Geographical Differences in Total and Pathogenic *Vibrio parahaemolyticus* and *Vibrio vulnificus* Levels in Seawater and Oysters from the Delaware and Chesapeake Bays Determined Using Several Methods. *Applied and*

environmental microbiology, 86(23), e01581-20. <https://doi.org/10.1128/AEM.01581-20>

18. Sangermani, M., Hug, I., Sauter, N., Pfohl, T., & Jenal, U. (2019). Tad Pili Play a Dynamic Role in *Caulobacter crescentus* Surface Colonization. *mBio*, 10(3), e01237-19. <https://doi.org/10.1128/mBio.01237-19>
19. Shime-Hattori, A., Iida, T., Arita, M., Park, K. S., Kodama, T., & Honda, T. (2006). Two type IV pili of *Vibrio parahaemolyticus* play different roles in biofilm formation. *FEMS microbiology letters*, 264(1), 89–97. <https://doi.org/10.1111/j.1574-6968.2006.00438.x>
20. Soto, W., & Nishiguchi, M. K. (2014). Microbial experimental evolution as a novel research approach in the Vibrionaceae and squid-Vibrio symbiosis. *Frontiers in microbiology*, 5, 593. <https://doi.org/10.3389/fmicb.2014.00593>
21. Tacket, C. O., Taylor, R. K., Losonsky, G., Lim, Y., Nataro, J. P., Kaper, J. B., & Levine, M. M. (1998). Investigation of the roles of toxin-coregulated pili and mannose-sensitive hemagglutinin pili in the pathogenesis of *Vibrio cholerae* O139 infection. *Infection and immunity*, 66(2), 692–695. <https://doi.org/10.1128/IAI.66.2.692-695.1998>
22. Velazquez-Roman, J., León-Sicairos, N., de Jesus Hernández-Díaz, L., & Canizalez-Roman, A. (2014). Pandemic *Vibrio parahaemolyticus* O3:K6 on the American continent. *Frontiers in cellular and infection microbiology*, 3, 110. <https://doi.org/10.3389/fcimb.2013.00110>
23. Watnick, P. I., Fullner, K. J., & Kolter, R. (1999). A role for the mannose-sensitive hemagglutinin in biofilm formation by *Vibrio cholerae* El Tor. *Journal of bacteriology*, 181(11), 3606–3609. <https://doi.org/10.1128/JB.181.11.3606-3609.1999>
24. Watnick, P. I., & Kolter, R. (1999). Steps in the development of a *Vibrio cholerae* El Tor biofilm. *Molecular microbiology*, 34(3), 586–595. <https://doi.org/10.1046/j.1365-2958.1999.01624.x>
25. Whitaker, W. B., Parent, M. A., Naughton, L. M., Richards, G. P., Blumerman, S. L., & Boyd, E. F. (2010). Modulation of responses of *Vibrio parahaemolyticus* O3:K6 to pH and temperature stresses by growth at different salt concentrations. *Applied and environmental microbiology*, 76(14), 4720–4729. <https://doi.org/10.1128/AEM.00474-10>

26. Zhong, X., Lu, R., Liu, F., Ye, J., Zhao, J., Wang, F., & Yang, M. (2021). Identification of LuxR Family Regulators That Integrate Into Quorum Sensing Circuit in *Vibrio parahaemolyticus*. *Frontiers in microbiology*, *12*, 691842. <https://doi.org/10.3389/fmicb.2021.691842>

Appendix A

BACTERIAL STRAINS AND PLASMIDS

Strains and plasmid	Description
<i>Vibrio parahaemolyticus</i> RIMD2210633	Wild type clinical isolate of <i>Vibrio parahaemolyticus</i> .
<i>Vibrio parahaemolyticus</i> Δ <i>mshA</i>	<i>Vibrio parahaemolyticus</i> with the <i>mshA</i> gene knocked out.
<i>Vibrio parahaemolyticus</i> Δ <i>rpoN</i>	<i>Vibrio parahaemolyticus</i> with the <i>rpoN</i> gene knocked out.
<i>Vibrio parahaemolyticus</i> Δ <i>opaR</i>	<i>Vibrio parahaemolyticus</i> with the <i>opaR</i> gene knocked out.
<i>Escherichia coli</i> β 2155 λ pir	<i>Escherichia coli</i> capable of taking up supercoiled DNA and conjugation.
<i>Escherichia coli</i> DH5 α	<i>Escherichia coli</i> capable of efficiently replicating large plasmids.
pDS132	Plasmid with <i>cat</i> and <i>sacB</i> gene that serves as a suicide vector.
pDS132 Δ VP2423	Pds132 vector with the Δ VP2423 AD DNA fragment inserted.

Table 1. A list of bacterial strains and plasmids used during the mutant making process.

Appendix B

PRIMERS USED IN MUTANT MAKING PROCESS

Primers	Sequence (5'->3')
$\Delta VP2423$ AB Forward	GTGGAATTCCCGGGAGAGCTGTATTAGTGCGTGTAGGAGAAATAAG
$\Delta VP2423$ AB Reverse	TATGGACAACGGCTCATAATGCTTAGCG
$\Delta VP2423$ CD Forward	ATTATGAGCCGTTGTCCATAAGTTTATCCCC
$\Delta VP2423$ CD Reverse	ACCGCATGCGATATCGAGCTGGTGATGTAGTAAAAGAAGTAGC
$\Delta VP2423$ Flanking Forward	CCAGCTGCGTTTTCTCAACT
$\Delta VP2423$ Flanking Reverse	TCGCAGTCACATAGTCACGA

Table 2. The table above displays the sequence of the primers used in the production of the $\Delta VP2423$ mutant.